

EEG ANALYSIS FOR DIGIT RECOGNITION BY TACTILE AND VIBROTACTILE STIMULATIONS

Anwasha Khasnobish^{1,a}, Shreyasi Datta^{2,b}, Dwaipayan Sardar^{2,c}, Amit Konar^{2,d}, Dewaki N. Tibarewala^{1,e}, Atulya K. Nagar^{3,f}

¹School of Bioscience and Engineering, ²Department of Electronics and Telecommunication Engineering,

³Department of Mathematics and Computer Science

^{1,2}Jadavpur University, ³Liverpool Hope University

^{1,2}Kolkata, India, ³United Kingdom

^aanweshakhasno@gmail.com, ^bshreyasidatta@gmail.com, ^cdsnalkel@gmail.com, ^dkonaramit@yahoo.co.in,

^ebiomed.ju@gmail.com, ^fnagara@hope.ac.uk

ABSTRACT

Artificial rehabilitative aids to enable object recognition to the disabled as well as robot aided and telenavigating systems require sending feedback signals to the human operator to enable accurate control. This work is a preliminary step towards the development of such systems using a Brain Computer Interface. In this work Electroencephalography (EEG) responses to tactile and vibrotactile stimulations, as alternate sensory means than vision, for recognizing ten digits, 0 to 9, has been studied. During tactile stimulation subjects are instructed to palpate digits embossed on plain surfaces, while vibrotactile stimulus is provided by vibrating motors attached to the subjects' skin over their clothing in specific patterns resembling the seven segment display of digits. EEG analysis involves feature extraction and classification into the respective digit classes. Correlation between the EEG features from the two stimulations is investigated and a nonlinear correlation is found to exist between them. A maximum classification accuracy of 73.17%, average over ten digit classes and all subjects under experimentation is observed for vibrotactually stimulated EEG analysis.

KEY WORDS

Brain Computer Interface, Electroencephalogram, Tactile Stimulus, Vibrotactile Stimulus

1. Introduction

Humans process various sensory stimuli to recognize objects and perceive the external world. The common sensory channels for object perception include vision, touch and hearing. In many neuro-motor or sensory motor diseases, the sense of object perception is lost or severely hampered because of the damage in any of the sensory abilities. Brain Computer Interface (BCI) based control of prosthetic aids, to assist the disabled, are associated with some form of feedback to the user for accurate control and communication [1-3]. BCI based assistance can be used in telenavigation or teleoperation using robotic aids as well, where object recognition by robots need to provide a feedback to the human operator in the form of a sensory

stimulus. Persons in need of a rehabilitative aid may have vision/hearing problems or paralysis, as in locked-in syndrome, such that the common sensory channels may not be usable for feedback. Again, in situations where object recognition is necessary in a multitasking environment such as gaming, the visual/auditory channels of the operator may be engaged in other activities. In such situations, tactile and vibrotactile [3-5] stimulations have proved to be an effective way of feedback in BCI problems. While tactile stimulation is simply the effect of touch, vibrotactile stimulation involves providing vibration patterns on the surface of the skin resembling the concerned objects.

Researchers have shown that objects can be identified from brain responses in the form of Electroencephalogram (EEG) [6], to visual and/or tactile stimuli depending on different parameters like shape, size, texture etc. [7-11]. Several receptors on the human skin can perceive mechanical vibrations and convey precise information to the central nervous system at a very high speed [5,12]. These include the slow adapting Merkel's receptors and the rapid adapting Meissner's corpuscles that provide high spatial resolution [5], Pacinian corpuscles that have large receptive fields and are quickly adapting [12] and the slow adapting Ruffini endings. Thus vibrotactile stimulus can also prove to be an effective technique for object identification. Various parameters determine the perception of vibrotactile stimulation; including the body part used, the frequency, the intensity (in terms of force) as well as the duration of vibration [5]. Vibrotactile stimulation based devices have been developed as alternative sensory means [13], for bypassing the necessity of audio feedback aiding the visually impaired with Braille knowledge [14], studying users' sensitivity to tactile apparent motion speed [15], spatial guidance [16], distinction of alphanumeric letters on the basis of vibrotactile stimulations [17] etc.

Based on the evidences of object recognition from brain signals upon suitable stimulation as mentioned above, the present work proposes to identify digits (0-9) from brain responses to tactile as well as vibrotactile stimulations. Tactile stimulations are provided in the form of plain surfaces embossed with the ten digit patterns those subjects have to palpate (explore dynamically with their

fingertips). Vibrotactile stimulation is arranged by attaching six vibrating DC motors on the subjects' skin surface over their clothing which vibrate in specific patterns so as to provide the sense of the ten digits according to the seven segment display format. While these stimulations are provided separately, the subjects' EEG signals are acquired, pre-processed for noise removal and are subjected to feature extraction and classification to recognize the ten digit classes, due to either type of stimulations. For EEG analysis, Adaptive Autoregressive Parameters [18-19], Successive signal differences [20] and Wavelet Transform [21-22] based features have been used along with Principal Component Analysis [29-30] for feature dimension reduction. Classification has been carried out using different standard pattern classifiers [23-24]. A nonlinear correlation has been revealed between the EEG features of the tactile and vibrotactile stimulations.

The rest of the paper is structured as follows. Section 2 covers the methodology followed with descriptions of the tools and techniques used. The experiments conducted have been elaborated in section 3. The results are discussed in section 4. Finally, in section 5 conclusions are drawn and the future scopes of work are stated.

2. Methodology

This section highlights the methodology followed along with the details of the various tools and techniques used for EEG processing and classification.

2.1 EEG Acquisition and Pre-Processing

EEG signals are acquired using a 21 channel Neurowin system [31] from Nasan Medical, at a sampling rate of 250Hz. For EEG acquisition, selection of the EEG modality, electrode positions and the frequency band are important factors.

2.1.1 Modality

Through a series of experiments, it is observed that followed by the tactile/vibrotactile stimuli presentation there is a desynchronization of the EEG signals followed by their synchronization. Thus event related desynchronization/synchronization (ERD/S) [7], [25] is considered as the EEG modality in the present work.

2.1.2 EEG Electrode Location and Frequency Band

Touch perception is related to the primary somatosensory cortex [9, 25-26]. Integration of the thought process, attention, and memory tasks is often related to the frontal lobe [27]. EEG signals from the parietal, frontal and motor cortex are of interest, which are acquired using scalp electrodes P3, P4, Pz; F3, F4, Fz; C3 and C4 placed according to the International 10-20 electrode system [25] as shown in Figure 1.

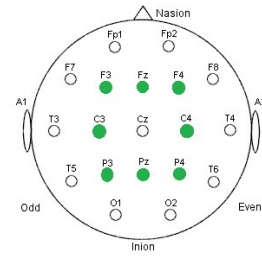


Figure 1. Electrode placement showing selected electrodes in green

EEG signals for somatosensory perception are especially significant in the theta band [28]. On performing Fourier Transform on the tactile as well vibrotactually stimulated EEG signals it is observed that maximum signal power content does not surpass the frequency range of 1-30Hz. An elliptical band pass filter, (because of its steeper transition characteristics compared to other types of filters) with bandwidth of 1-30Hz is implemented for extracting the denoised EEG signals.

2.1.3 Spatial Filtering

To eliminate inter-channel interference, spatial filtering [7] is implemented through common average referencing. In this technique, for data from each EEG channel, that from all the channels equally weighted are subtracted. This eliminates the commonality of the data from that channel with the rest and preserves its specific temporal features.

2.2 Feature Extraction

To represent the EEG signals with reduced dimension while producing maximum discrimination between the various digit patterns, different features are extracted from the pre-processed EEG.

2.2.1 Adaptive Autoregressive Parameters

Autoregressive Parameters and Adaptive Autoregressive Parameters (AAR) are time-domain features for EEG analysis [18-19]. In AAR model, the AR parameters for representing EEG signals are estimated in a time-varying manner, as explained by (1) and (2), where the index j is an integer to denote discrete, equidistant time points, $y(j)$ is the j^{th} instance of the signal, p is the order of the AAR model, $y(j-i)$ with $i = 1$ to p are the p previous sample values, $a_{i,j}$ are the time-varying AR model parameters, and $x(j)$ is a zero-mean-Gaussian-noise process with time varying variance $\sigma_x^2(j)$.

$$y(j) = a_{1,j}y(j-1) + \dots + a_{p,j}y(j-p) + x(j) \quad (1)$$

$$x(j) = N\{0, \sigma_x^2(j)\} \quad (2)$$

There are various algorithms to estimate the AAR parameters such as, Least Mean Squares, Kalman filtering,

Recursive AR or Recursive Least Squares [18]. After trials with different model orders, it is found that the best results are obtained in most cases with order 6 and hence AAR order 6 is computed, using Kalman Filtering as the estimation algorithm. The AAR parameters are adapted with an update coefficient of 0.0085, set heuristically.

2.2.2 Wavelet Features

Wavelet transform [21] provides both frequency as well as time-domain analysis of a signal at multiple resolutions. In Discrete Wavelet Transform signals are passed through filters, high pass and low pass, in several stages. At each stage i , each filter output is down sampled by two to produce the approximation coefficient A_i and the detail coefficient D_i . The approximation coefficient is then decomposed again, to get the approximation and detail coefficients of the subsequent stages. The desired level of transform and which coefficients are to be selected as the features are determined by the required frequency range. Wavelet coefficients as features generally result in high dimensional feature spaces and hence suitable feature selection techniques are used there. In this work Principal Component Analysis (PCA) has been used to reduce the feature space dimension and select the best features based on eigen value decomposition [29-30].

Apart from the use of the wavelet coefficients directly as features, some features on the wavelet coefficients can be computed that produce smaller feature space. This scheme is termed as a ‘lifting scheme’ in literature [22]. Seven features (WLift) have been computed on the wavelet coefficients that resulted in good discrimination between the classes. These are four statistical features, namely Mean, Standard Deviation, Skewness and Kurtosis; and Power, Entropy (WE) and Recursing Energy Efficiency (WREE) of the wavelet coefficients. WREE is a measure of the ratio of the energy of the wavelet coefficients of a particular frequency band to the total energy content of all levels and is given by (3) where E_i denotes the energy of the i^{th} band/level of decomposition and E_{total} is the total energy of all the bands. Entropy is a measure of the information content in the signal. WE is calculated using (4) where $WREE_i$ is the WREE at level i , for a total of M levels of decomposition.

$$WREE_i = \frac{E_i}{E_{total}} \quad (3)$$

$$WE_i = -\sum_{i=1}^M WREE_i \log(WREE_i) \quad (4)$$

In order to evaluate the wavelet coefficients in the frequency range as determined by the EEG power spectrum, wavelet approximate coefficients (WAPP) at the third level of decomposition are computed as features using Daubechies (order 4) mother wavelet. WREE and WE are computed with respect to this level of decomposition. For wavelet coefficients the number of selected features per electrode is fixed at 50 (tactile EEG) and 300 (vibrotactile EEG) using PCA.

2.2.3 Signal Differences

In order to capture the variations in the temporal characteristics in the EEG signals, the differences of the signal amplitudes at consecutive instants of time have been considered as time domain features [20]. First and second order differences (D1 and D2) have been considered in this work. For a discrete EEG signal $y(j)$ at the j^{th} instant, these are computed using (5) and (6), where $y'(j)$ and $y''(j)$ denote the first and second order differences respectively.

$$y'(j) = y(j+1) - y(j) \quad (5)$$

$$y''(j) = y'(j+1) - y'(j) \quad (6)$$

Such feature spaces have dimensions in the order of $L-1$ and $L-2$ respectively for a length of EEG of L and as the length L is usually a large number because of the large number of EEG samples produced per second, the feature dimensions are reduced using PCA [29-30] to obtain the best features and the number of selected features is fixed at 800 (tactile EEG) and 2000 (vibrotactile EEG) per electrode, by trial and error, on observing the best performance on an average for each type of stimulation.

Feature extraction is performed for each electrode separately and then these are normalized and concatenated to obtain the total feature space in each case. Normalization is done by (7) where $f_{i,j}$ denotes the j^{th} instance of the i^{th} feature and $f_{i,max}$ and $f_{i,min}$ denote the maximum and minimum values of that feature respectively.

$$f_{i,j} \leftarrow \frac{f_{i,j} - f_{i,min}}{f_{i,max} - f_{i,min}} \quad (7)$$

2.3 Classification

Standard pattern classification algorithms are used to discriminate the stimulated EEG responses, namely, Support Vector Machine (SVM) [23-24] Radial Basis Function (RBF) as well as Polynomial kernel, k -Nearest Neighbour (k -NN) [23-24] and Naïve Bayes classifier [23-24]. SVM is used with RBF and Polynomial kernels as linear SVM is generally not suitable for BCI problems [23]. All the algorithms are based on supervised machine learning principle, that is, the classifiers are trained on a sample dataset and then implemented on the test dataset. The training and testing data sets are determined by 5-fold cross-validation. Classification is carried out in a one-vs.-all basis taking each digit as one class and the rest as the other class. SVMs have been tuned with a cost value of 100, determined experimentally. The width of the Gaussian for RBF kernel is taken as 1 and the order and constant term of the polynomial as 2 and 0 respectively for polynomial kernel. These values are determined after noting the best performances after several trials. The Naive Bayes classifier is used with the assumption that the features have a normal distribution whose mean and

covariance are learned during the process of training. For k NN, experiments are conducted by varying the distance metric as well as the value of ' k ' or the number of nearest neighbours to be considered. In most of the cases Euclidean distance with $k=3$ produced the best results and hence these parameters are used along with Majority Voting as the voting mechanism to determine the class of the test samples.

Classification accuracy (CA), Sensitivity and Specificity as calculated from the confusion matrices [32] are considered as metrics for performance analysis. All these metrics should approach 1 for good classification. The Receiver Operating Characteristics (ROC) [32] denotes the variation of the true positive rate (Sensitivity) in the y -axis with the false positive rate (1 - Specificity) in the x -axis. The area under the ROC curve is termed as AUC [32] and is also used as a performance metric.

2.4 Correlation Analysis between EEG Responses from Tactile and Vibrotactile Stimulations

Though instances of EEG based object recognition from tactile stimulus exists [10], there is no such evidence in case of vibrotactile stimulation to the best of the authors' knowledge. To prove that vibrotactile stimulation can generate patterns specific to objects that can be recognized from EEG, a relation is tried to establish between the features from tactually and vibro-tactually stimulated EEG. From the computation of Pearson's linear correlation coefficient [33], no conclusive proof of the existence of a linear relation can be obtained. Hence a nonlinear correlation [34-35] between the features is investigated by computing non-linear correlation coefficient (NCC).

3. Experimental Paradigm

3.1 Material Preparation for Tactile Stimulus

Plain surfaces (2.5cm×2cm) are embossed with hard acrylic paint that produces digits 0 to 9 with depth of about 1mm in seven segment digital display format (Figure 2). The digits span 2cm and 1cm respectively along the length and breadth. The top left corner of each surface is embossed with a dot for keeping track of the orientation of the digit. Subjects palpate these embossed digits repeatedly to understand them during tactile stimulus presentation.



Figure 2. Embossed digits

3.2 Vibrotactile Pattern Generation

Vibrotactile displays can be made from vibrating DC motors [36]. In this work, six coin vibration motors, named M1 to M6, as shown in Figure 3 are placed on the back of subjects following specific arrangement, similar to seven

segment display format, so as to represent the ten digits 0 to 9. The small DC motors used in the work have unbalanced loads in their rotors, whose rotation cause the motors to vibrate upon electrical excitation [36]. The intensity of vibration is proportional to the input voltage while the output frequency is constant. In this study the distance between every motor pair is set to 60mm to produce better discriminability in vibration patterns, as assessed from the subjects' response. As such amount of distance upon a flat surface is conveniently available on the subject's back; we have selected it for motor placement. Though the spatial resolution of the back is better than 60mm [37], this distance is necessary to provide correct discrimination between the digit patterns in the present context of experimentations. In order to provide vibrotactile sensation corresponding to the 10 digits, the motors are activated sequentially according to the patterns shown in Figure 4.

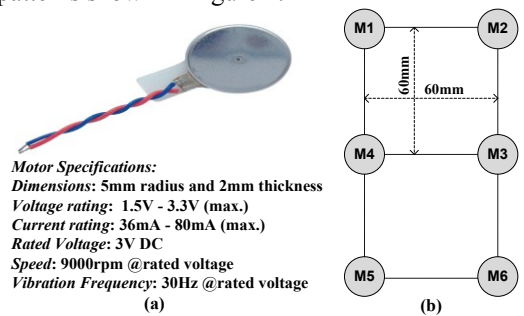


Figure 3. (a) DC motor used in the experiments and (b) Arrangement of motors in seven segment display format

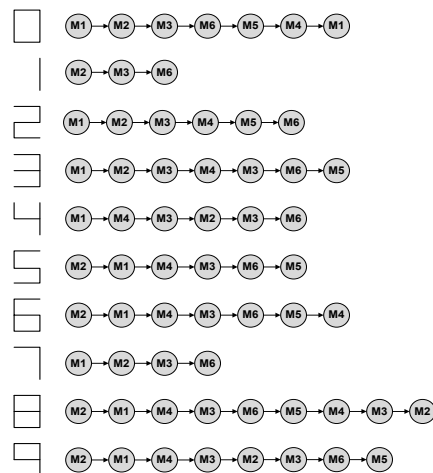


Figure 4. Vibration sequence of the motors for generating vibrotactile stimulus corresponding to the 10 digits

Square pulses are generated to actuate the vibration motors in specific sequence and timing to ensure proper vibrotactile display of the digits to the subjects. The delay between onset of consecutive square pulses (T_D), the on-duration of a particular square pulse (T_{ON}), as well as the spatial arrangement of the vibrating motors, control the feeling of the stimulus to be continuous and smooth such that the necessary patterns are properly conveyed and understood [38]. For generating these square wave

patterns, a general purpose microcontroller unit (MCU), the AtMega16 [39], a microcontroller with an 8-bit embedded processor, enclosing various peripheral features has been used. The processor is operated at a frequency of 8MHz and programmed prior to experimentation in order to set the values of durations of delay (T_D) and overlap (T_I) to 324ms and 107ms respectively, and hence $T_{ON} = T_D + T_I$ is 431ms. These values are set by trial and error to make the subjects understand the patterns properly. Input is provided to the MCU in the form of on/off switches to indicate the sequence of pattern to be generated, i.e. for each of the 10 patterns there is a switch. For each pattern the corresponding combination of the control signals are fired.

An example of control signal generation for digit-1, depicting a series of square wave pulses is illustrated in Figure 5. The motors are actuated in the form of a 'Delayed Chain Sequence'. First, the motor M2 is turned on followed by a delay of T_D before turning on the next motor, (i.e. M3, in this example). After a delay of T_I (T_I denoting the overlap duration between two consecutive motors), control for M2 is turned off. The next motor, i.e. M6, is turned on T_D delay after turning on motor M3. This sequence is followed, i.e. each control is turned on, and after T_D delay the next control is turned on, the previous is kept on for another T_I delay. When all the motor controls required for the pattern are switched on once, an epoch ends and is equal to $d = (NMC+1)*T_D + T_I$ where NMC is the number of motor controls required for that pattern. A cycle is of duration $4*d$. At the end of the first cycle, a delay is applied and the cycle is repeated for a second time. The values of T_D and T_I are constant however, the duration of vibration for a particular digit (0 to 9) is dependent upon the number of motors necessary for that particular digit pattern generation.

The square wave control signals generated by the MCU need to be power amplified before they can actually drive the motors. The interfacing of each of the MCU generated signals with the respective motors is done using a transistor based driver circuit. Each driver circuit draws power from a 3.5 V voltage regulator and provides outputs in the range 3-3.2V and 30-78mA which lie within the voltage and current specifications of the motors.

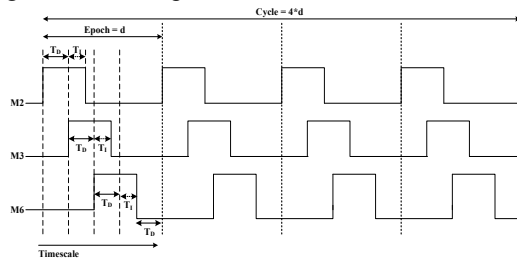


Figure 5. Timing diagram for generation of pattern for '1'

3.3 Subjects

Eight healthy subjects, four male and four female, in the age group 25 ± 3 years, participate in the experiments after signing consent forms.

3.4 Stimulus Presentation

The presentation of stimulus follows the sequence depicted in Figure 6(a). Figure 6(b) shows the experimental setup for vibrotactile stimulation.

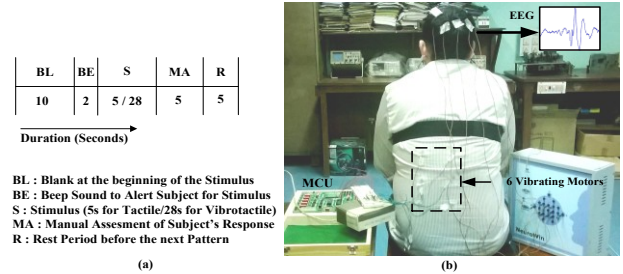


Figure 6. (a) Stimulus pattern and (b) Experimental setup for vibrotactile stimulation

Data is acquired from the subjects in blindfolded condition. Ten seconds of rest is used to bring the EEG signals to the base level at the beginning. For each sample a beep sound alerts the subject of the start of the stimulus. Next the digit is presented to the subject either in the form of tactile stimulation by embossed surface patterns or by vibrotactile stimulation using the vibrating motors. From the subjects' feedbacks it is found that 5 seconds is sufficient for any of the embossed digit recognition from tactile stimulus. For the vibrotactile stimulus, taking $T_D=324ms$, $T_I=107ms$, the time required for pattern '8' is the largest, (as it requires the maximum number of motor controls) and a little less than 28 seconds. The stimulus duration, fixed at 28 seconds, is kept constant for all patterns. In case of the other patterns that complete epochs before that of '8', the number of repetitions is increased in such a way that the stimulus duration remains the same. At the end of the stimulation each subject is instructed to say the digit that he/she understood from the stimulation for manual assessment of the subject's understanding. A period of 5 seconds of rest then precedes the pattern for the next sample. For tactile stimulation, an instance is of 5 seconds duration. For vibrotactile stimulation the duration of each stimulus is longer. From each stimulus of 28s duration, EEG data of as many instances as the number of repetitions of a vibration cycle, are acquired using windows of appropriate lengths. In each type of the stimulations, 10 instances of each class of data acquired from each subject are processed.

4. Results and Discussions

4.1 Classification Results

The one vs. all classification accuracies of each digit class D for tactile and vibrotactile EEGs are reported in Table 1 and Table 2 respectively. In all the tables, the mean classification accuracy (CA) and the standard deviation SD (in parenthesis) over the 8 subjects are shown.

Table 1
Mean CA in % (\pm SD) from Tactile Stimulated EEG

D ^f	Features				
	AAR ^a	WAPP ^b	WLift ^c	D1 ^d	D2 ^e
0	71.25 (\pm 0.06)	66.00 (\pm 0.03)	72.75 (\pm 0.05)	63.25 (\pm 0.03)	68.50 (\pm 0.04)
1	74.75 (\pm 0.04)	69.25 (\pm 0.04)	73.00 (\pm 0.05)	65.25 (\pm 0.03)	70.25 (\pm 0.03)
2	68.75 (\pm 0.08)	67.50 (\pm 0.04)	69.25 (\pm 0.09)	64.25 (\pm 0.03)	68.75 (\pm 0.04)
3	70.25 (\pm 0.07)	65.75 (\pm 0.03)	66.25 (\pm 0.07)	62.25 (\pm 0.03)	69.50 (\pm 0.03)
4	69.25 (\pm 0.08)	69.50 (\pm 0.04)	73.25 (\pm 0.05)	64.75 (\pm 0.03)	70.00 (\pm 0.03)
5	70.25 (\pm 0.06)	66.00 (\pm 0.05)	69.75 (\pm 0.09)	64.75 (\pm 0.03)	69.75 (\pm 0.03)
6	75.50 (\pm 0.05)	68.75 (\pm 0.04)	66.50 (\pm 0.08)	64.00 (\pm 0.05)	69.00 (\pm 0.04)
7	67.50 (\pm 0.07)	67.50 (\pm 0.05)	72.75 (\pm 0.05)	65.25 (\pm 0.03)	71.25 (\pm 0.05)
8	74.00 (\pm 0.04)	66.25 (\pm 0.05)	69.00 (\pm 0.03)	61.75 (\pm 0.03)	69.25 (\pm 0.03)
9	66.50 (\pm 0.08)	65.50 (\pm 0.06)	65.75 (\pm 0.07)	63.25 (\pm 0.04)	68.75 (\pm 0.04)

^aAdaptive Autoregressive Parameters, ^bApproximate Wavelet Coefficients, ^cLifted Wavelet Features, ^dFirst order temporal difference, ^eSecond order temporal difference, ^fDigit/Class

Table 2
Mean CA in % (\pm SD) from Vibrotactile Stimulated EEG

D ^f	Features				
	AAR ^a	WAPP ^b	WLift ^c	D1 ^d	D2 ^e
0	73.25 (\pm 0.02)	72.50 (\pm 0.02)	71.00 (\pm 0.08)	72.25 (\pm 0.06)	72.00 (\pm 0.03)
1	71.75 (\pm 0.02)	74.25 (\pm 0.02)	76.25 (\pm 0.03)	74.00 (\pm 0.06)	72.25 (\pm 0.03)
2	74.50 (\pm 0.01)	74.50 (\pm 0.02)	68.50 (\pm 0.07)	69.25 (\pm 0.06)	71.75 (\pm 0.04)
3	73.50 (\pm 0.01)	74.25 (\pm 0.02)	71.00 (\pm 0.05)	68.00 (\pm 0.08)	72.75 (\pm 0.03)
4	73.50 (\pm 0.02)	74.50 (\pm 0.02)	75.25 (\pm 0.06)	72.25 (\pm 0.06)	71.75 (\pm 0.04)
5	73.00 (\pm 0.02)	71.75 (\pm 0.06)	71.50 (\pm 0.09)	73.25 (\pm 0.06)	72.25 (\pm 0.04)
6	73.75 (\pm 0.02)	72.00 (\pm 0.05)	66.00 (\pm 0.06)	69.50 (\pm 0.07)	69.75 (\pm 0.04)
7	74.25 (\pm 0.02)	72.25 (\pm 0.05)	74.00 (\pm 0.06)	74.00 (\pm 0.05)	71.25 (\pm 0.04)
8	72.50 (\pm 0.02)	70.75 (\pm 0.05)	69.75 (\pm 0.06)	68.50 (\pm 0.05)	73.50 (\pm 0.04)
9	71.75 (\pm 0.02)	71.00 (\pm 0.05)	67.75 (\pm 0.08)	69.50 (\pm 0.08)	68.25 (\pm 0.06)

^aAdaptive Autoregressive Parameters, ^bApproximate Wavelet Coefficients, ^cLifted Wavelet Features, ^dFirst order temporal difference, ^eSecond order temporal difference, ^fDigit/Class

From the above tables it is clearly observed that vibrotactile stimulation performs better for digit classification from EEG on an average, achieving a highest of 73.17% accuracy over all classes with AAR features. The plots of ROC along with the AUC values for a particular class (digit '1'), as positive class in OVA classification using k NN ($k=3$) classifier for Subject 1 is illustrated in Figure 7. For tactile stimulation the point (0.3, 0.6) on the ROC curve indicates sensitivity of 60% and specificity of 70% while for vibrotactile stimulation the point (0, 0.6) indicates sensitivity 60% and specificity 100%.

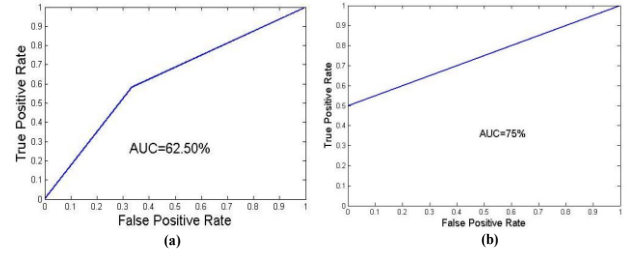


Figure 7. Sample ROC plots with AUC values for class 1 (Wavelet Approximate Coefficient features) as positive class in OVA classification with 3-NN classifier for (a) Tactile Stimulus and (b) Vibrotactile Stimulus

4.2 Classifier Performance Assessment

In order to evaluate efficiency of the classifiers used and find the best, their performances are compared. Friedman Test [40] is conducted to rank the classifiers on the basis of mean classification accuracies (CA). The null hypothesis states that all the classifiers are equivalent and hence their ranks R_j should be equal. The Friedman statistic, distributed according to $K-1$ degrees of freedom is given by (8), where, K is the number of classification algorithms and N is the number of datasets respectively.

$$\chi_F^2 = \frac{12N}{K(K+1)} \left[\sum_j R_j^2 - \frac{K(K+1)^2}{4} \right] \quad (8)$$

Table 3
Friedman Test

Classifier / EEG Type		k -NN ^a ($k=3$)	SVM ^b RBF	SVM ^c Polynomial	Naive Bayes
Tactile	Mean CA (%)	71.20	70.85	66.35	65.53
	Mean Rank	1.25	1.75	3.25	3.63
Vibrotactile	Mean CA (%)	73.17	71.30	66.42	69.67
	Mean Rank	1.25	1.88	3.88	3

^a k -Nearest Neighbour classifier, ^bSupport Vector Machine with Radial Basis Function kernel, ^cSupport Vector Machine with Polynomial kernel

In this work $K=4$ and $N=8$ (for 8 subjects). The classifiers ranked on the basis of the best mean one vs. all (over the different features) classification accuracies over all datasets are tabulated in Table 3. Using these ranks, χ_F^2 is calculated by (8) to be 16.15 and 19.92 for tactile and vibrotactile EEG classifications respectively. These are greater than $\chi_{3,0.95}^2 = 7.815$ that indicate the null hypothesis to be correct to an extent of 5%. Hence, the null hypothesis claiming the equivalence of all classifiers fails, and they are ranked by their classification accuracies.

4.3 Non-Linear Correlation Assessment

As the feature dimensions for AAR and WLift are the same for both the EEG (tactile and vibrotactile), Linear Correlation Coefficient (LCC) and NCC are evaluated for

only these features. The absolute values of LCC must be near unity for perfect covariance, either positive or negative. However, obtained LCC values (feature-wise) always lie below 0.5. The average of the feature-wise NCC values (evaluated according to the method in [34-35] taking 5 ranks), for each of these feature spaces over all classes for each subject is above 0.5 denoting the existence of a non linear correlation in between the tactually and the vibrotactually stimulated EEG. The mean values and the standard deviations (in parenthesis) of the LCC and NCC over all subjects are reported for 4 randomly selected digit classes in Table 4.

Table 4
LCC and NCC Values for AAR and WLift Features

Class	LCC ^a		NCC ^b	
	AAR ^c	WLift ^d	AAR ^c	WLift ^d
'1'	0.1105 (±0.22)	0.1665 (±0.26)	0.6558 (±0.13)	0.6277 (±0.08)
'3'	0.1587 (±0.42)	0.1920 (±0.34)	0.6196 (±0.15)	0.5693 (±0.08)
'5'	0.2355 (±0.37)	0.3025 (±0.42)	0.6276 (±0.10)	0.8277 (±0.16)
'7'	0.1225 (±0.45)	0.2925 (±0.35)	0.7213 (±0.11)	0.6473 (±0.07)

^aLinear Correlation Coefficient, ^bNon-Linear Correlation Coefficient, ^cAdaptive Autoregressive Parameters, ^dLifted Wavelet Features

4.4 Assessment of Subjects' Verbal Responses

The subjects' verbal responses show commendable accuracy in perceiving the tactile/vibrotactile stimulations to recognize the 10 digits. The percentage of correct responses over all instances of a particular class, average over all the subjects is reported in Figure 8.

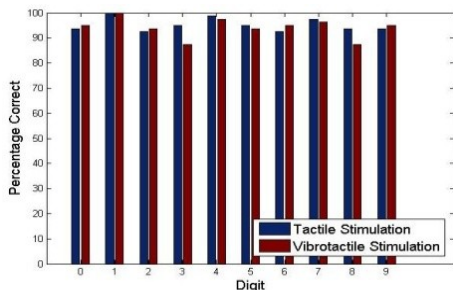


Figure 8. Average percentage of correct verbal responses over all instances of a particular class

5. Conclusion

The present work successfully illustrates the classification of EEG signals in response to tactile as well as vibrotactile stimulations for digit recognition. The study is validated from the analysis of results from 8 healthy subjects who palpate embossed digits as tactile stimulus and feel vibrotactile stimulus in patterns of the seven segment display through vibration motors attached on their back in

blindfolded conditions. Manual assessment of the subjects' verbal responses of the stimuli is also done to determine whether the subject could understand the stimulus. It is found that individually vibrotactile stimuli are better for recognition of digits from EEG.

The present work can be extended in the future for applications in the development of alternative sensory means based artificial rehabilitative aids to enable digit recognition to the paralyzed/visually disabled. After extensive performance evaluation, it can also be useful in robot aided telenavigating systems that must send feedback signals to a human operator in a multitasking environment with the operator's visual/auditory channels engaged in other activities.

Acknowledgement

This study has been supported by University Grants Commission, India, University of Potential Excellence Program (UGC-UPE) (Phase II) in Cognitive Science, Jadavpur University and Council of Scientific and Industrial Research (CSIR), India.

References

- [1] J. R. Wolpaw, N. Birbaumer, D. J. McFarland, G. Pfurtscheller & T. M. Vaughan, Brain-computer interfaces for communication and control, *Clinical Neurophysiology*, 113(6), 2002, 767-791.
- [2] A. B. Schwartz, X. T. Cui, D. J. Weber & D. W. Moran, Brain-controlled Interfaces: Movement Restoration with Neural Prosthetics, *Neuron*, 52(1), 2006, 205-220.
- [3] L. Kauhainen, T. Palomäki, P. Jylänki, F. Aloise, Marnix Nuttin & J. del R. Millan, Haptic feedback compared with visual feedback for BCI, *Proc. 3rd International BCI Workshop and Training Course*, 2006, 66-67.
- [4] A. Chatterjee, V. Aggarwal, A. Ramos, S. Acharya & N.V. Thakor, A Brain Computer Interface with Vibrotactile biofeedback for Haptic Information, *Journal of NeuroEngineering and Rehabilitation*, 4(1), 2007, 1-12.
- [5] F. Cincotti et al, Vibrotactile feedback for brain-computer interface operation, *Computational Intelligence and Neuroscience*, 2007, 2007, 1-12.
- [6] E. A. Curran & M. J. Stokes, Learning to control brain activity: a review of the production and control of EEG components for driving brain-computer interface (BCI) systems, *Brain and Cognition*, 51(3), 2003, 326-336.
- [7] G. Dornhege, *Towards brain-computer interfacing* (MIT Press, 2007).
- [8] J. Martinovic, R. Lawson & M. Craddock, Time course of information processing in visual and haptic object classification, *Frontiers in human neuroscience*, 6, 2012.
- [9] M. Grunwald, *Human haptic perception* (Boston Basel Berlin: Birkhaeuser Verlag AG, 2008).
- [10] A. Khasnobish, A. Konar, D. N. Tibarewala, S. Bhattacharyya, and R. Janarthanan, Object Shape Recognition from EEG Signals during Tactile and Visual Exploration, *Proc. Pattern Recognition and Machine Intelligence, Springer Berlin Heidelberg*, 2013, 459-464.

- [11] S. Datta, A. Saha & A. Konar, Perceptual Basis of Texture Classification from tactile stimulus by EEG Analysis, *Proc. National Conference on Brain and Consciousness*, Kolkata, 2013, 38-45.
- [12] R. S. Johansson, U. Landstrom & R. Lundstrom, Responses of mechanoreceptive afferent units in the glabrous skin of the human hand to sinusoidal skin displacements, *Brain research*, 244(1), 1982, 17-25.
- [13] K. A. Kaczmarek, J. G. Webster, P. Bach-y-Rita & W. J. Tompkins, Electrotactile and vibrotactile displays for sensory substitution systems, *IEEE Transactions on Biomedical Engineering*, 38(1), 1991, 1-16.
- [14] H. Nicolau, J. Guerreiro, T. Guerreiro & L. Carriço, UbiBraille: designing and evaluating a vibrotactile Braille-reading device, *Proc. 15th International ACM SIGACCESS Conference on Computers and Accessibility*, 2013, 1-8.
- [15] L. Kohli, M. Niwa, H. Noma, K. Susami, Y. Yanagida, R. W. Lindeman, K. Hosaka & Y. Kume, Towards effective information display using vibrotactile apparent motion, *Proc. 2006 14th Symposium on Haptic Interfaces for Virtual Environment and Teleoperator Systems*, 2006, 445-451.
- [16] B. Weber, S. Schatzle, T. Hulin, C. Preusche & B. Deml, Evaluation of a vibrotactile feedback device for spatial guidance, *Proc. World Haptics Conference (WHC)*, 2011, 349-354.
- [17] Y. Yanagida, M. Kakita, R. W. Lindeman, Y. Kume & N. Tetsutani, Vibrotactile letter reading using a low-resolution tactor array, *Proc. 12th International Symposium on Haptic Interfaces for Virtual Environment and Teleoperator Systems*, 2004, 400-406.
- [18] A. Schlögl, The electroencephalogram and the adaptive autoregressive model: theory and applications, Germany: Shaker, 2000.
- [19] H. Nai-Jen & R. Palaniappan, Classification of mental tasks using fixed and adaptive autoregressive models of EEG signals, *Proc. 2nd International Conference of the IEEE EMBS on Neural Engineering*, 2005, 633-636.
- [20] C. Chatfield, *The analysis of time series, an introduction*, sixth edition (New York: Chapman & Hall/CRC, 2004).
- [21] E. D. Übeyli, Combined neural network model employing wavelet coefficients for EEG signals classification, *Digital Signal Processing*, 19(2), 2009, 297-308.
- [22] A. Khasnobish, S. Bhattacharyya, A. Konar, D.N. Tibarewala, S.D. Burman & R. Janarthan, Positive and Negative Emotion Classification from Stimulated EEG signals, In *Biomedical Engineering*, (R.R. Galigeke, A.G Ramakrishnan, J.K., Udupa (Eds), New Delhi: Narosa Publishing House, 2012) 114-119.
- [23] F. Lotte, M. Congedo, A. Lécuyer, F. Lamarche & B. Arnaldi, A review of classification algorithms for EEG-based brain-computer interfaces, *Journal of neural engineering*, 4(2), 2007.
- [24] Tom M. Mitchell, *Machine learning* (McGraw Hill, 1997).
- [25] M. Teplan, Fundamentals of EEG measurement, *Measurement Science Review*, 2(2), 2002, 1-11.
- [26] C. Preuschhof, H. R. Heekeren, B. Taskin, T. Schubert & A. Villringer, Neural correlates of vibrotactile working memory in the human brain, *The Journal of Neuroscience*, 26(51), 2006, 13231-13239.
- [27] J. S. Kim, O. L. Kim, W. S. Seo, B. H. Koo, Y. Joo & D. S. Bai, Memory Dysfunctions after Mild and Moderate Traumatic Brain Injury: Comparison between Patients with and without Frontal Lobe Injury, *Journal of Korean Neurosurgical Society*, 46(5), 2009, 459-467.
- [28] M. Grunwald, T. Weiss, W. Krause, L. Beyer, R. Rost, I. Gutberlet & Hermann-Josef Gertz, Theta power in the EEG of humans during ongoing processing in a haptic object recognition task, *Cognitive Brain Research*, 11(1), 2001, 33-37.
- [29] F. Song, Z. Guo & Dayong Mei, Feature selection using principal component analysis, *Proc. 2010 IEEE International Conference on System Science, Engineering Design and Manufacturing Informatization (ICSEM)*, vol.1, 2010, 27-30.
- [30] A. Halder, A. Jati, G. Singh, A. Konar, A. Chakraborty, & R. Janarthan, Facial Action Point Based Emotion Recognition by Principal Component Analysis, *Proc. International Conference on Soft Computing for Problem Solving (SocProS 2011)*, 2011, 721-733.
- [31] www.nasanmedical.com
- [32] T. Fawcett, An introduction to ROC analysis, *Pattern recognition letters*, 27(8), 2006, 861-874.
- [33] N. G. Das, *Statistical Methods* (TataMcGrawHill, 2008).
- [34] Q. Wang, Y. Shen and J. Q. Zhang, A nonlinear correlation measure for multivariable data set, *Physica D: Nonlinear Phenomena*, 200(3), 2005, 287-295.
- [35] A. Khasnobish, S. Datta, M. Pal, A. Konar, D. N. Tibarewala & R. Janarthan, Correlation Analysis of Object Shape Recognition from EEG and Tactile Signals, *Proc. IEEE International Conference in Advances in Electrical Engineering (ICAEE) 2014*, Vellore, India, January 2014.
- [36] M. Niwa, Y. Yanagida, H. Noma, K. Hosaka & Y. Kume, Vibrotactile apparent movement by DC motors and voice-coil tactors, *Proc. 14th International Conference on Artificial Reality and Telexistence (ICAT)*, 2004, 126-131.
- [37] J. van Erp, Vibrotactile spatial acuity on the torso: effects of location and timing parameters, *Eurohaptics Conference, 2005 and Symposium on Haptic Interfaces for Virtual Environment and Teleoperator Systems, 200, World Haptics 2005*.
- [38] M. Niwa, R. W. Lindeman, Y. Itoh & F. Kishino, Determining appropriate parameters to elicit linear and circular apparent motion using vibrotactile cues, *Proc. World Haptics 2009-Third Joint EuroHaptics conference and Symposium on Haptic Interfaces for Virtual Environment and Teleoperator Systems*, 2009, 75-78.
- [39] www.atmel.in
- [40] J. Demsar, Statistical comparisons of classifiers over multiple data sets, *The Journal of Machine Learning Research*, 7, 2006, 1-30.